




# Excellent piezoelectric performance of Bi-compensated 0.69BiFeO<sub>3</sub>-0.31BaTiO<sub>3</sub> lead-free piezoceramics

Wenbin Yi<sup>1</sup>, Zhenya Lu<sup>1,\*</sup> , Xingyue Liu<sup>1</sup>, Du Huang<sup>1</sup>, Zhi Jia<sup>1</sup>, Zhiwu Chen<sup>1</sup>, Xin Wang<sup>1</sup>, and Huixiang Zhu<sup>2</sup>

<sup>1</sup>School of Materials Science and Engineering, South China University of Technology, Guangzhou 510640, China

<sup>2</sup>Guangzhou Kailitech Electronics Co., Ltd, Guangzhou 511356, China

Received: 29 March 2021

Accepted: 1 August 2021

Published online:  
14 August 2021

© The Author(s), under exclusive licence to Springer Science+Business Media, LLC, part of Springer Nature 2021

## ABSTRACT

This work focuses on the effects of Bi compensation on the phase structure, microstructure, ferroelectric, and piezoelectric performances of new 0.69Bi<sub>1+x</sub>FeO<sub>3</sub>-0.31BaTiO<sub>3</sub> ( $x$ , 0–0.08) piezoceramics fabricated by traditional sintering techniques. X-ray diffraction (XRD) results indicated that Bi compensation has slight influences on the phase structure and all the ceramics locate near the morphotropic phase boundary of rhombohedral–pseudocubic phase coexistence. The rhombohedral phase fraction of all the ceramics fluctuates slightly in the range of 41.7–49.1 %. X-ray photoelectron spectroscopy (XPS) results confirmed that Bi compensation favors the decrease in the percentage of oxygen vacancy in the ceramics. An appropriate content of Bi compensation facilitates the densification, grain growth as well as enhancement of piezoelectric property of the materials. In addition, Bi compensation makes the materials “soft” along with the lower  $E_C$  compared with the no compensation ceramics. Significantly, the excellent piezoelectric performance ( $d_{33} = 207$  pC/N) was achieved in the 0.69Bi<sub>1.04</sub>FeO<sub>3</sub>-0.31BaTiO<sub>3</sub> ceramics, which is higher than the results obtained in the previously reported BiFeO<sub>3</sub>-BaTiO<sub>3</sub>-based ceramics. This work would trigger further study on the BiFeO<sub>3</sub>-BaTiO<sub>3</sub>-based piezoceramics for practical application.

## 1 Introduction

Piezoceramics with the ability to convert mechanical energy to electrical energy and vice versa have been used as core materials to manufacture actuators, transducers, and sensors [1]. However, according to the Restriction of Hazardous Substances legislation, the conventional Pb(Zr, Ti)O<sub>3</sub> (PZT)-based

piezoceramics which dominate the market have faced serious challenges due to the toxicity of lead element to the human health and natural environment, promoting extensive studies on perovskite lead-free piezoceramics [1, 2].

Recently, lead-free BiFeO<sub>3</sub>-BaTiO<sub>3</sub> (BF–BT) system piezoceramics, as a promising substitute for PZT-based ceramics, have received much attention due to

Address correspondence to E-mail: zhylu@scut.edu.cn

its high Curie temperature  $T_C$  and good piezoelectric performance [1–4]. In general, three approaches such as the chemical doping or composition design [4–7], processing optimization (quenching or sintering in special atmosphere) [2, 8–11], and using novel starting materials (nano-BaTiO<sub>3</sub> powder) [3, 12–14] were used to enhance the piezoelectric performance of BF–BT ceramics. To be specific, the value of piezoelectric coefficient  $d_{33}$  for the most BF–BT ceramics with only chemical doping or composition design is below 195 pC/N [1, 15, 16]. Significantly, the outstanding  $d_{33}$  of 402 pC/N was achieved in the 0.67Bi<sub>1.05</sub>Fe<sub>0.97</sub>Ga<sub>0.03</sub>O<sub>3</sub>–0.33BaTiO<sub>3</sub> ceramics [2] via water quenching following sintering, which gave rise to a rapid surge of studies [1, 12–14, 17, 18] on the BF–BT-based ceramics. However, the quenching process may lead to much microcracks in the ceramics due to the extremely fast cooling rate following sintering [12], which might be unsuitable for mass production. Besides, it was reported that the improved  $d_{33}$  up to 191–214 pC/N [3, 12–14] was obtained in BF–BT ceramics using nano-BaTiO<sub>3</sub> powder as starting materials. But, the cost of nano-BaTiO<sub>3</sub> powders is much higher compared with the total cost of ordinary TiO<sub>2</sub> and BaCO<sub>3</sub> powders.

On the other hand, Bi<sup>3+</sup> and Pb<sup>2+</sup> cations have the same valence shell electron configuration 6s<sup>2</sup>6p<sup>0</sup>. It is believed that the strong ferroelectricity and piezoelectricity of BiScO<sub>3</sub>–PbTiO<sub>3</sub> are mainly ascribed to the onset of hybridization between Bi/Pb-6p and O-2p orbitals [19]. Similarly, super high ferroelectric polarization (90–100 μC/cm<sup>2</sup>) was predicted in BF owing to the hybridization between Bi-6p and O-2p orbitals [14, 20]. However, it is known that Bi is prone to volatilize during sintering at high temperatures, which may cause the deviation from the stoichiometric composition for BF-based ceramics [21]. As reported, appropriately excess Bi<sub>2</sub>O<sub>3</sub> has positive effects on the piezoelectric property of BF–BT materials. It was also confirmed that the enhanced  $d_{33}$  was achieved in the other Bi-based piezoceramics (e.g., Bi<sub>0.5</sub>Na<sub>0.5</sub>TiO<sub>3</sub>) [22, 23] by means of excess Bi<sub>2</sub>O<sub>3</sub>. Unfortunately, the improved  $d_{33}$  of 114 pC/N [24] and 142 pC/N [21] of BF–BT with excess Bi<sub>2</sub>O<sub>3</sub> are not very excellent. Therefore, it is necessary to further study the influences of Bi compensation on the electrical property of BF–BT system piezoceramics.

In our previous investigation of undoped BF–BT series solid solution piezoceramics, it was found that the optimal piezoelectric activity was obtained in the

ceramics with BF/BT molar ratio of 0.69/0.31 [25]. In this work, Bi-compensated 0.69Bi<sub>1+x</sub>FeO<sub>3</sub>–0.31BaTiO<sub>3</sub> (B<sub>1+x</sub>F-0.31BT) ceramics, using ordinary BaCO<sub>3</sub>, TiO<sub>2</sub>, Bi<sub>2</sub>O<sub>3</sub>, and Fe<sub>2</sub>O<sub>3</sub> powder as raw materials, were fabricated by conventional sintering techniques without quenching. The effects of Bi compensation on the phase structure, ferroelectric, and piezoelectric performances of B<sub>1+x</sub>F-0.31BT ceramics near morphotropic phase boundary (MPB) were systematically investigated. As expected, excellent piezoelectric property ( $d_{33} = 207$  pC/N) was achieved in the ceramics with an appropriate content ( $x = 0.04$ ) of Bi compensation, which is superior to the results obtained in the previously reported BF–BT-based piezoceramics.

## 2 Experimental procedure

B<sub>1+x</sub>F-0.31BT ( $x, 0-0.08$ ) ceramics were synthesized via conventional sintering techniques. The starting materials with high purity (> 99 %) including Fe<sub>2</sub>O<sub>3</sub>, Bi<sub>2</sub>O<sub>3</sub>, TiO<sub>2</sub>, and BaCO<sub>3</sub> were weighed and milled in an alcohol with ZrO<sub>2</sub> balls for 12 h. After drying to remove alcohol, the mixtures were calcined at 800 °C for 3 h followed by second ball milling for 12 h. The powders were dried and pressed with 1 % PVA under 100 MPa into pellets with 14 mm diameter and ~ 1.30 mm thickness. After burning off the binder at 600 °C for 2 h, the pellets were sintered in a sealed crucible at 1020 °C for 3 h. Silver slurry was pasted on both faces of the sintered pellets and then fired at 580 °C for 20 min. The samples were poled under a dc field of 5 kV/mm in a silicone oil bath at 90 °C for 30 min and approximately 24 h after poling, piezoelectric parameters were measured.

X-ray diffraction (XRD, X' Pert Pro, PANalytical, the Netherlands) was used to characterize the phase structure. The scanning electron microscopy (SEM, NOVA NANOSEM 430, the Netherlands) was used to observe the microstructure of the ceramics. The bulk density of B<sub>1+x</sub>F-0.31BT ceramics was evaluated by the Archimedes method. X-ray photoelectron spectroscopy (XPS, Axis Ultra DLD, Kratos, UK) with Al K $\alpha$  radiation was used to analyze the state of oxygen in the ceramics. A ferroelectric analyzer (Radiant Technologies, USA) was used to measure the room-temperature polarization–electric ( $P$ – $E$ ) hysteresis loops at 1 Hz. The piezoelectric coefficient  $d_{33}$  was measured by a piezo- $d_{33}$  meter (ZJ-3 A, China).

The dielectric permittivity  $\epsilon_r$  and dielectric loss  $\tan\delta$ , mechanical quality factors  $Q_{mv}$  and planar mechanical coupling coefficient  $k_p$  were measured using an impedance analyzer 4294 A (Agilent Technologies, America).

### 3 Results and discussion

Figure 1 presents the room-temperature XRD patterns of  $B_{1+x}F-0.31BT$  ceramics. It can be seen that the ceramics with  $x = 0$  and  $x = 0.02$  possess pure perovskite structure, while the impurity phase peak of  $Bi_{25}FeO_{40}$  can be observed for the ceramics with  $x \geq 0.04$ . This indicates that excess Bi compensation could give rise to the impurities phase in  $B_{1+x}F-0.31BT$  ceramics, which is consistent with the observation of the impurity phase  $Bi_{25}FeO_{40}$  in the 0.70BF-0.30BT ceramics with 0.03–0.05 Bi compensation [14]. In order to further analyze the influences of Bi compensation on the phase structure of  $B_{1+x}F-0.31BT$  materials, a general diffraction/reflectivity analysis program MAUD [26] was used to perform full-pattern matching with the Rietveld method. The values of the goodness-of-fit indicator  $S$  (1.53–1.70) and reliability  $R_{wp}$  (12.2–13.7 %), as shown in Table 1, are less than 2 and 15 %, respectively, suggesting that the calculated and observed XRD patterns are matched well [26]. All the  $B_{1+x}F-0.31BT$  samples locate near

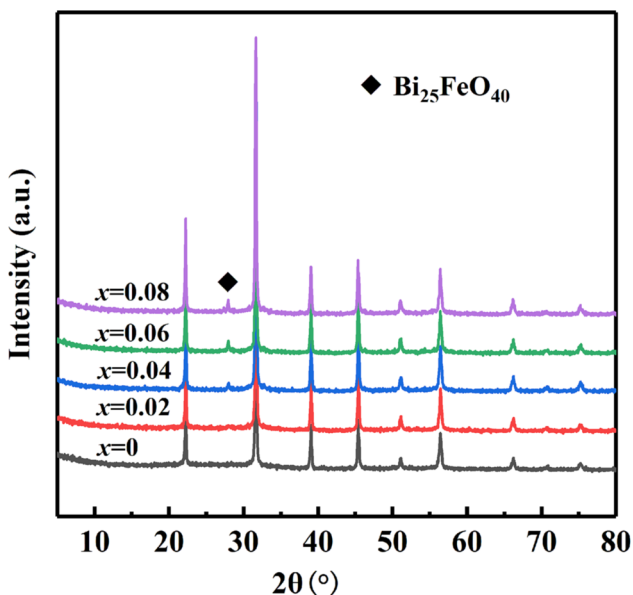


**Fig. 1** Room-temperature XRD patterns of  $B_{1+x}F-0.31BT$  ceramics

MPB of rhombohedral (R)–pseudocubic (pC) phase coexistence, and R phase fraction fluctuates in the range of 41.7–49.1 % as shown in Table 1. The similar MPB of R-pC coexistence was also reported in 0.70BF-0.30BT ceramics [3, 27]. In addition, the differences in crystal lattice  $a$  and  $\alpha$  of the  $B_{1+x}F-0.31BT$  ceramics are insignificant. These results indicate that no remarkable variation in main phase structure is caused by Bi compensation in the  $B_{1+x}F-0.31BT$  ceramics, namely, Bi compensation has ignorable effects on the main phase structure of BF–BT materials [14, 21, 24].

The surface microstructure of  $B_{1+x}F-0.31BT$  ceramics is given in Fig. 2. The  $B_{1+x}F-0.31BT$  ceramics with Bi compensation of  $x = 0.02$  and  $x = 0.04$  exhibit dense microstructure and clear grain boundaries, while the ceramics with Bi compensation of  $x = 0.06$  and  $x = 0.08$  present looser grain boundaries. The improved relative density, as shown in Table 1, of 96.8 and 96.5 % is obtained for  $x = 0.02$  and  $x = 0.04$  ceramics, respectively. These results imply that an appropriate concentration of Bi compensation is beneficial to densification of the ceramics, which facilitates the electrical property enhancement for the ceramics. The grain size of  $B_{1+x}F-0.31BT$  increases firstly and then decreases slightly, for example, 5.8, 7.5, 7.7, 9.8, and 9.0  $\mu m$  for  $x$  of 0, 0.02, 0.04, 0.06, and 0.08, respectively. This could be ascribed to the low melting point (830  $^{\circ}C$ ) of  $Bi_2O_3$ . Thus, an appropriate amount of liquid phase can be formed during sintering for the ceramics with Bi compensation of  $x \leq 0.06$ , which favors the diffusion of elements in the  $B_{1+x}F-0.31BT$  solid solutions, resulting in the larger grain size. However, too much liquid phase caused by excess Bi compensation could assemble at grain boundaries, which may suppress the grain growth during sintering [4, 24].

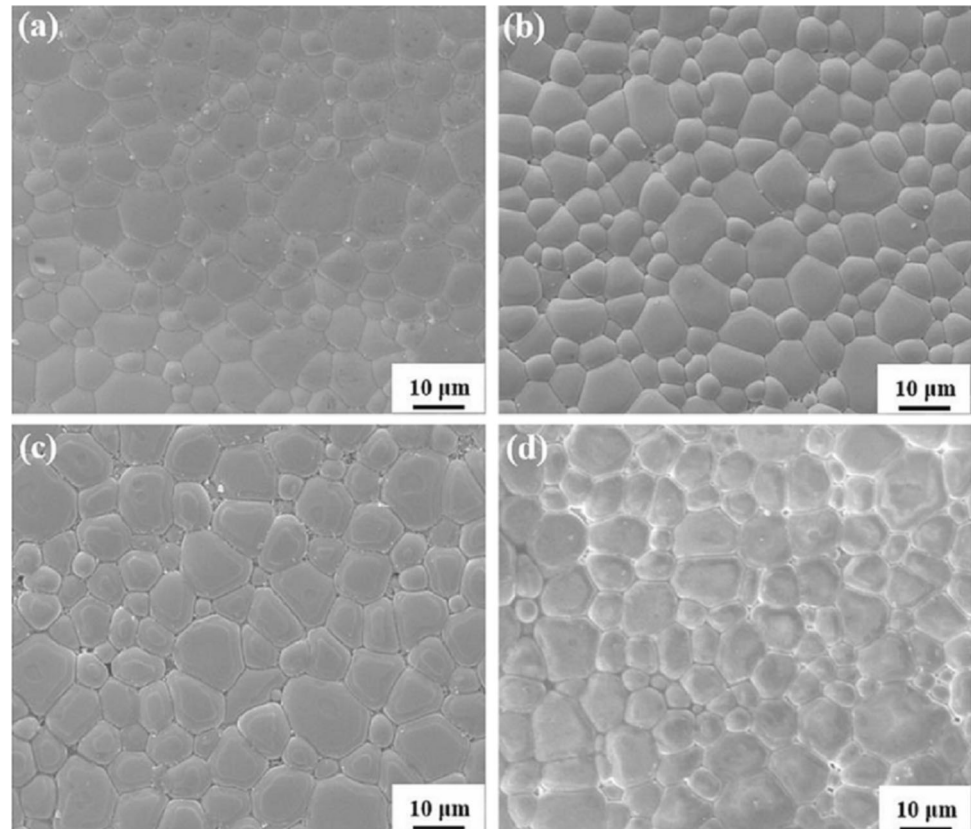
Figure 3 displays the temperature dependence of dielectric permittivity  $\epsilon_r$  and dielectric loss  $\tan\delta$  of  $B_{1+x}F-0.31BT$  ceramics at 100 kHz. A typical dielectric anomaly, corresponding to the Curie peak, is observed for all the  $B_{1+x}F-0.31BT$  samples from room temperature to 550  $^{\circ}C$ . The Curie temperature  $T_C$  of all the  $B_{1+x}F-0.31BT$  samples lies in the range of 439–454  $^{\circ}C$ . Besides, the  $\tan\delta$  of all the  $B_{1+x}F-0.31BT$  ceramics almost remain stable till 370  $^{\circ}C$  and then increases dramatically near 450  $^{\circ}C$  due to high-temperature leakage conduction. Note that the  $T_C$  of the conventional PZT ceramics is in the range of 190–370  $^{\circ}C$  [1], severely limiting its application at

**Table 1** Fitting parameters ( $S$  and  $R_{wp}$ ), lattice parameters, and relative density of  $B_{1+x}F-0.31BT$  ceramics

$x$ (mol)	Lattice parameters		Weight* (%)	R-factors		Relative density (%)
	$a = b = c$ (Å)	$\alpha = \beta = \gamma$ (°)		$R_{wp}$ (%)	$S$	
0	3.9966(6)	89.84	49.1 <sup>R</sup>	12.24	1.53	95.7
	3.9935(3)	–	50.9 <sup>pC</sup>			
0.02	3.9963(9)	89.85	48.6 <sup>R</sup>	12.9	1.6	96.8
	3.9937(6)	–	51.4 <sup>pC</sup>			
0.04	3.9966(1)	89.83	41.6 <sup>R</sup>	13.51	1.68	96.5
	3.9941(1)	–	58.4 <sup>pC</sup>			
0.06	3.9967(8)	89.84	44.5 <sup>R</sup>	13.63	1.69	95.5
	3.9934(4)	–	55.5 <sup>pC</sup>			
0.08	3.9969(8)	89.85	41.7 <sup>R</sup>	13.7	1.7	95.8
	3.9928(9)	–	58.3 <sup>pC</sup>			

\* <sup>R</sup> Rhombohedral, <sup>pC</sup> Pseudocubic.

**Fig. 2** SEM images of  $B_{1+x}F-0.31BT$  ceramics with  $x = 0.02$  (a),  $x = 0.04$  (b),  $x = 0.06$  (c), and  $x = 0.08$  (d)



high temperature. According to the above results,  $B_{1+x}F-0.31BT$  ceramics would have promising potential application at high temperature.

The  $P$ – $E$  hysteresis loops of  $B_{1+x}F-0.31BT$  ceramics at 1 Hz and room temperature are presented in Fig. 4a. All the ceramics exhibit typical  $P$ – $E$  loops, and Bi compensation plays an important role in both the  $P_r$  and  $E_C$  of  $B_{1+x}F-0.31BT$  samples. With increasing the content of Bi compensation, the  $P_r$

decreases gradually from  $24.09 \mu\text{C}/\text{cm}^2$  for  $x = 0$  to  $18.55 \mu\text{C}/\text{cm}^2$  for  $x = 0.08$  as shown in Fig. 4b, and  $E_C$  decreases firstly from  $24.98 \text{ kV}/\text{cm}$  for  $x = 0$  to  $22.63 \text{ kV}/\text{cm}$  for  $x = 0.06$  and then slightly increases to  $23.28 \text{ kV}/\text{cm}$  for  $x = 0.08$ . It is known that the Bi evaporation could lead to the formation of A-site and oxygen vacancies in the  $ABO_3$ -type perovskite solid solutions; and through pinning at ferroelectric domain walls, the oxygen vacancy could inhibit the

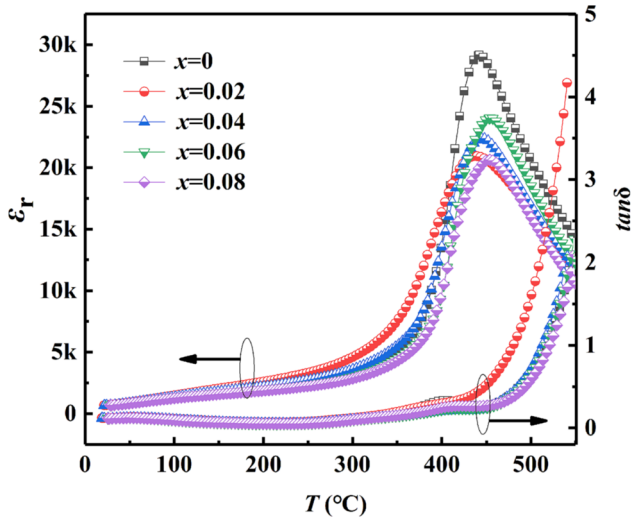


**Fig. 3** Temperature dependence of dielectric permittivity  $\epsilon_r$  and loss  $\tan\delta$  of  $B_{1+x}F-0.31BT$  ceramics at 100 kHz

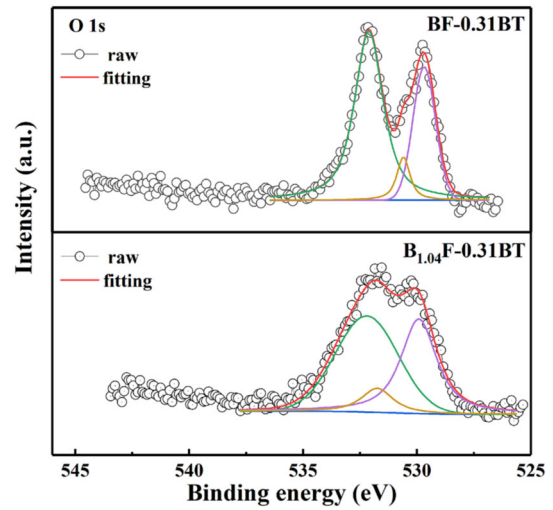


**Fig. 5** XPS spectra of O 1 s of the BF-0.31BT and  $B_{1.04}F-0.31BT$  ceramics

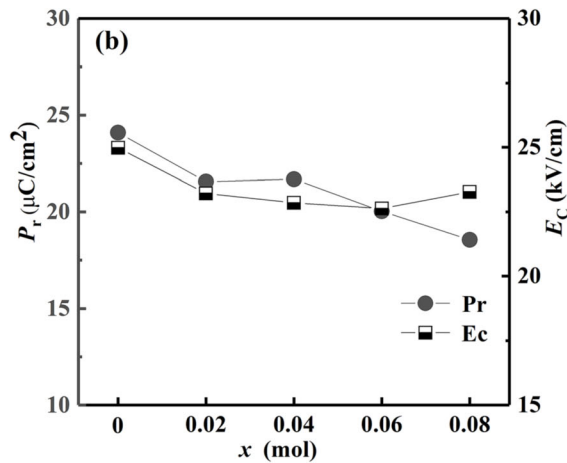
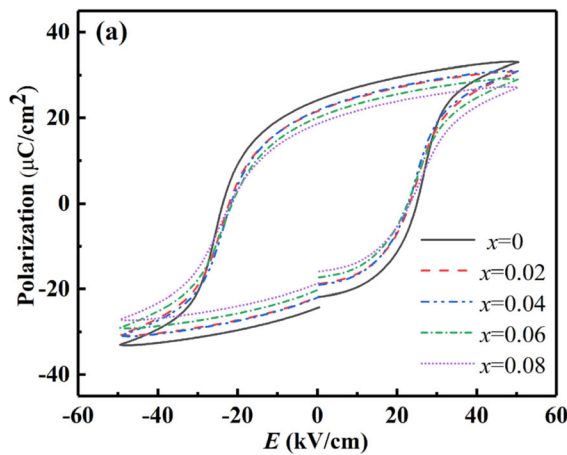


**Fig. 4**  $P-E$  hysteresis loops of  $B_{1+x}F-0.31BT$  ceramics at 1 Hz (a); remnant polarization  $P_r$  and coercive field  $E_C$  of  $B_{1+x}F-0.31BT$  ceramics as a function of  $x$  (b)

reorientation of domains during electric poling [12, 28]. Figure 5 shows XPS spectra of O 1 s of the ceramics. The three-fitted sub-peaks at  $\sim 529$  eV,  $\sim 531$  eV, and  $\sim 532$  eV correspond to the lattice oxygen, adsorbed  $H_2O$ , and oxygen vacancy, respectively [29]. As shown in Table 2, the oxygen vacancy percentage is 63.3 and 51.1 % for BF-0.31BT and  $B_{1.04}F-0.31BT$ , respectively. This confirms that Bi compensation favors the decrease of oxygen vacancy in the ceramics, which facilitates the reorientation of the ferroelectric domains of  $B_{1+x}F-0.31BT$  ceramics. Similar phenomenon of the decreased percentage of oxygen vacancy in BF-BT ceramics via adding excess  $Bi_2O_3$  was also reported by Zheng et al. [29].

**Table 2** Fitted peaks of O 1 s of the ceramics

O 1 s	Peaks	Atomic (%)
BF-0.31BT	532.1	63.3
	530.6	7.6
	529.7	29.1
$B_{1.04}F-0.31BT$	532.4	51.1
	531.6	8.9
	530.1	40.0

Moreover, the improved relative density and the larger grain size as mentioned in Fig. 2 are also in favor of the domain reorientation [12]. Therefore, the

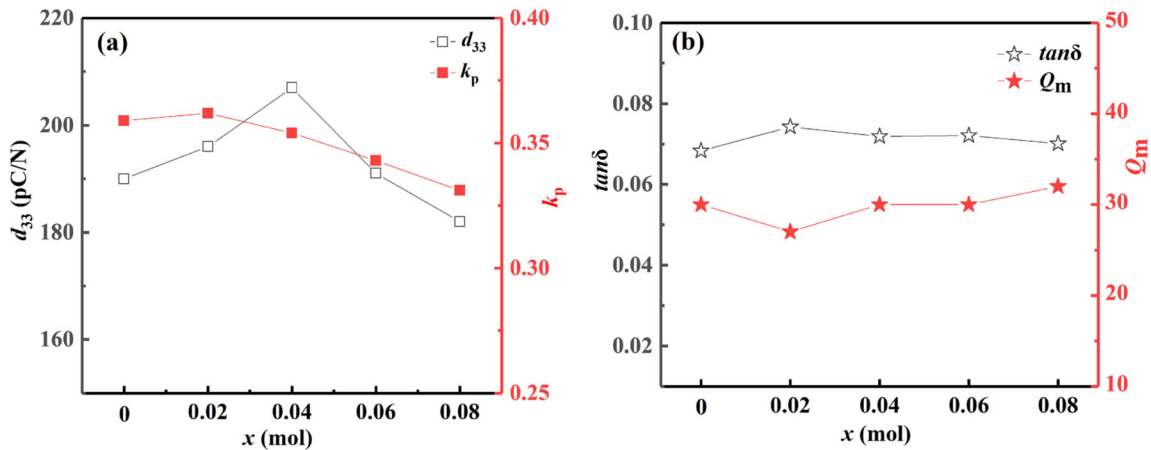


**Fig. 6** Piezoelectric coefficient  $d_{33}$  and planar electromechanical coupling factor  $k_p$  (a) and dielectric loss  $\tan\delta$  and mechanical quality factor  $Q_m$  (b) of  $B_{1+x}F-0.31BT$  ceramics

lower  $E_C$  is observed for the ceramics with Bi compensation compared with the no compensation ceramics. In other words, Bi compensation could make the  $B_{1+x}F-0.31BT$  ceramics “soft” to some extent.

Figure 6a presents the piezoelectric coefficient  $d_{33}$  and planar electromechanical coupling factor  $k_p$  of  $B_{1+x}F-0.31BT$  ceramics. Both the  $d_{33}$  and  $k_p$  of the samples increase firstly and then decrease as  $x$  increases. For example, the  $d_{33}$  value increases from 190 pC/N for  $x = 0$  to 207 pC/N for  $x = 0.04$  and then decreases to 182 pC/N for  $x = 0.08$ , and the value of  $k_p$  increases from 0.359 for  $x = 0$  to 0.362 for  $x = 0.02$  and then decreases to 0.331 for  $x = 0.08$ . These results reveal that a proper content of Bi compensation is beneficial for the improvement of piezoelectric performances. The reason for the enhancement of  $d_{33}$  may be mainly contributed to the decreased  $E_C$  as shown in Fig. 4b of  $B_{1+x}F-0.31BT$  with an appropriate concentration of Bi compensation. However, the ceramics with excess Bi compensation ( $x = 0.08$ ) show inferior  $d_{33}$ , although the  $E_C$  of  $B_{1.08}F-0.31BT$  is lower than that of the ceramics without Bi compensation. This should be owing to the severe deteriorated  $P_r$  for the  $B_{1.08}F-0.31BT$  ceramics. Nevertheless, it is necessary to note that all the samples possess the relatively high piezoelectric properties ( $d_{33}$ , 182–207 pC/N,  $k_p$ , 0.33–0.36), which should be attributed to the formed MPB in the experimental range as above XRD results. The dielectric loss  $\tan\delta$  and mechanical quality factors  $Q_m$  of  $B_{1+x}F-0.31BT$  samples are displayed in Fig. 6b. Generally, Bi compensation has slight effects on both the  $\tan\delta$  and  $Q_m$

of  $B_{1+x}F-0.31BT$  ceramics. Specifically, the  $\tan\delta$  and  $Q_m$  of the samples fluctuate in the range of 0.068–0.074 and 27–32, respectively.

The piezoelectric property of recently reported non-quenched BF–BT system piezoceramics are listed in Table 3. Significantly, the excellent piezoelectric property ( $d_{33} = 207$  pC/N) is obtained in the  $B_{1.04}F-0.31BT$  ceramics in this work, which is higher than those of 0.75BiFeO<sub>3</sub>-0.25BaTiO<sub>3</sub>-0.1 wt% MnO<sub>2</sub> (116 pC/N) [9], 0.7BiFeO<sub>3</sub>-0.3BaTiO<sub>3</sub>-1 mol% MnO<sub>2</sub> (177 pC/N) [10], 0.7Bi(Fe<sub>0.991</sub>Zn<sub>0.009</sub>)O<sub>3</sub>-0.3BaTiO<sub>3</sub>-0.3 wt% MnO<sub>2</sub> (192 pC/N) [15], and 0.7BiFeO<sub>3</sub>-0.3BaTiO<sub>3</sub>-0.025BiZn<sub>0.5</sub>Ti<sub>0.5</sub>O<sub>3</sub>-0.003Li<sub>2</sub>CO<sub>3</sub>-0.0035MnO<sub>2</sub> (184 pC/N) [16] and even higher or comparable with the results ( $d_{33} = 191 \sim 214$  pC/N) obtained in 0.70BF-0.30BT ceramics [3, 12–14] using costly nano-BaTiO<sub>3</sub> powder as starting materials. Considering positive effects of chemical doping or composition design on piezoelectric property of BF–BT materials, further enhanced piezoelectric performance could be obtained in the ceramics based on  $B_{1.04}F-0.31BT$  through composition optimization or adding optimal dopants.

## 4 Conclusion

The  $B_{1+x}F-0.31BT$  ( $x$ , 0–0.08) piezoceramics were prepared via ordinary sintering techniques. All the ceramics with different concentrations of Bi compensation locate near MPB of R-pC phase coexistence. A trace amount of impurity phase was detected for the materials, when  $x \geq 0.04$ . The R/pC

**Table 3** Piezoelectric property and phase structure of recently reported BiFeO<sub>3</sub>-BaTiO<sub>3</sub> ceramics

Composition	Raw materials	Sintering atmosphere	Phase structure	$Q_m$	$d_{33}$ (pC/N)	$k_p$	Ref.
0.75BiFeO <sub>3</sub> -0.25BaTiO <sub>3</sub> -0.1 wt% MnO <sub>2</sub>	Ordinary	O <sub>2</sub>	R-pC	–	116	–	[9]
0.70BiFeO <sub>3</sub> -0.30BaTiO <sub>3</sub> -1.0 mol% MnO <sub>2</sub>	Ordinary	O <sub>2</sub>	R-pC	–	177	0.37	[10]
0.71BiFe <sub>0.97</sub> (Mg <sub>0.5</sub> Ti <sub>0.5</sub> ) <sub>0.03</sub> O <sub>3</sub> -0.29BaTiO <sub>3</sub> - 0.6 wt% MnO <sub>2</sub>	Ordinary	Air	pC	–	155	~ 0.28	[6]
0.65BiFeO <sub>3</sub> -0.35BaTiO <sub>3</sub> -0.6 wt%MnO <sub>2</sub> - 0.4 wt% CuO	Ordinary	Air	pC	–	170	~ 0.33	[5]
0.70BiFeO <sub>3</sub> -0.30BaTiO <sub>3</sub>	Ordinary	Air	R-pC	–	134	0.29	[27]
0.7Bi(Fe <sub>0.991</sub> Zn <sub>0.009</sub> )O <sub>3</sub> -0.3BaTiO <sub>3</sub> - 0.3 wt% MnO <sub>2</sub>	Ordinary	Air	R	–	192	0.31	[15]
0.7BiFeO <sub>3</sub> -0.3BaTiO <sub>3</sub> -0.025BiZn <sub>0.5</sub> Ti <sub>0.5</sub> O <sub>3</sub> - 0.003Li <sub>2</sub> CO <sub>3</sub> -0.0035MnO <sub>2</sub>	Ordinary	Air	R	35	184	0.36	[16]
0.70BiFeO <sub>3</sub> -0.30BaTiO <sub>3</sub>	Nano-BaTiO <sub>3</sub>	Air	R-pC	26	210	0.34	[3]
0.70BiFeO <sub>3</sub> -0.30BaTiO <sub>3</sub>	Ordinary	Air	R-pC	37	164	0.31	[3]
0.70BiFeO <sub>3</sub> -0.30BaTiO <sub>3</sub>	Nano-BaTiO <sub>3</sub>	Air	R-T	~ 28	208	0.35	[12]
0.70BiFeO <sub>3</sub> -0.30BaTiO <sub>3</sub>	Nano-BaTiO <sub>3</sub>	Air	R-T	~ 30	191	0.35	[13]
0.70Bi <sub>1.02</sub> FeO <sub>3</sub> -0.30BaTiO <sub>3</sub>	Nano-BaTiO <sub>3</sub>	Air	R-pC	~ 24	214	0.35	[14]
0.69Bi <sub>1.04</sub> FeO <sub>3</sub> -0.31BaTiO <sub>3</sub>	Ordinary	Air	R-pC	30	207	0.35	This work

phase ratio fluctuates slightly in the range of 41.7/58.3–49.1/50.9 % for all the ceramics. An appropriate content of Bi compensation could facilitate the densification and grain growth of the samples. Decreased percentage of oxygen vacancy was observed for  $x = 0.04$  compared with the no compensation ceramics as confirmed by XPS results. The  $T_C$  fluctuates in the range of 439 to 454 °C for the ceramics with increasing  $x$  to 0.08. Bi compensation, exhibiting “soft” doping effects, favors the decrease of  $E_C$  of the ceramics. Owing to the increased relative density, larger grain size, and decreased  $E_C$ , the excellent piezoelectric performance ( $d_{33} = 207$  pC/N) was obtained for the B<sub>1.04</sub>F-0.31BT ceramics, which would inspire further investigation on BF–BT system piezoceramics for practical application.

### Acknowledgements

This work was supported by the R & D Projects in Key Fields of Guangdong Province (2020B0109380001; 2019B040403004; 2019B040403006); Science and Technology Planning Project of Guangxi Zhuang Autonomous Region (No. AA18118034);

National Natural Science Foundation of China (Grant No.51577070 and U1601208); Science and Technology Program of Guangzhou (No. 201704030095).

### Data availability

The data and material will be provided under reasonable request.

### Declarations

**Conflict of interest** The authors have no known competing financial interests or personal relationships that could have appeared to influence the work reported in this paper.

### References

1. T. Zheng, J. Wu, D. Xiao, J. Zhu, Prog. Mater Sci. **98**, 552–624 (2018)
2. M.H. Lee, D.J. Kim, J.S. Park, S.W. Kim, T.K. Song, M.H. Kim, W.J. Kim, D. Do, I.K. Jeong, Adv. Mater. **27**, 6976–6982 (2015)

3. S. Cheng, L. Zhao, B.P. Zhang, K.K. Wang, *Ceram. Int.* **45**, 10438–10447 (2019)
4. D. Lin, Q. Zheng, Y. Li, Y. Wan, Q. Li, W. Zhou, *J. Eur. Ceram. Soc.* **33**, 3023–3036 (2013)
5. H. Yang, C. Zhou, X. Liu, Q. Zhou, G. Chen, W. Li, H. Wang, *J. Eur. Ceram. Soc.* **33**, 1177–1183 (2013)
6. C. Zhou, A. Feteira, X. Shan, H. Yang, Q. Zhou, J. Cheng, W. Li, H. Wang, *Appl. Phys. Lett.* **101**, 032901 (2012)
7. S. Murakami, N.T.A.F. Ahmed, D. Wang, A. Feteira, D.C. Sinclair, I.M. Reaney, *J. Eur. Ceram. Soc.* **38**, 4220–4231 (2018)
8. T. Zheng, J. Wu, *J. Alloy. Compd.* **676**, 505–512 (2016)
9. S.O. Leontsev, R.E. Eitel, *J. Am. Ceram. Soc.* **92**, 2957–2961 (2009)
10. J. Wei, D. Fu, J. Cheng, J. Chen, *J. Mater. Sci.* **52**, 10726–10737 (2017)
11. Q. Li, J. Cheng, J. Chen, *J. Mater. Sci. Mater. Electron.* **28**, 1370–1377 (2016)
12. L.F. Zhu, B.P. Zhang, J.Q. Duan, B.W. Xun, N. Wang, Y.C. Tang, G.L. Zhao, *J. Eur. Ceram. Soc.* **38**, 3463–3471 (2018)
13. L.F. Zhu, B.P. Zhang, Z.C. Zhang, S. Li, L.J. Wang, L.J. Zheng, *J. Mater. Sci.: Mater. Electron.* **29**, 2307–2315 (2018)
14. B.W. Xun, N. Wang, B.P. Zhang, X.Y. Chen, Y.Q. Zheng, W.S. Jin, R. Mao, K. Liang, *Ceram. Int.* **45**, 24382–24391 (2019)
15. K. Tong, C. Zhou, Q. Li, J. Wang, L. Yang, J. Xu, G. Chen, C. Yuan, G. Rao, *J. Eur. Ceram. Soc.* **38**, 1356–1366 (2018)
16. Y. Sun, H. Yang, S. Guan, Y. Cao, M. Jiang, X. Liu, Q. Chen, M. Li, J. Xu, *J. Alloy. Compd.* **819**, 153058 (2020)
17. T. Zheng, Y. Ding, J. Wu, *J. Mater. Sci. Mater. Electron.* **28**, 11534–11542 (2017)
18. Q. Li, J. Wei, T. Tu, J. Cheng, J. Chen, *J. Am. Ceram. Soc.* **100**, 5573–5583 (2017)
19. J. Íñiguez, D. Vanderbilt, L. Bellaiche, *Phys. Rev. B* **67**, 224107 (2003)
20. J.B. Neaton, C. Ederer, U.V. Waghmare, N.A. Spaldin, K.M. Rabe, *Phys. Rev. B* **71**, 014113 (2005)
21. C. Zhou, H. Yang, Q. Zhou, G. Chen, W. Li, H. Wang, *J. Mater. Sci. Mater. Electron.* **24**, 1685–1689 (2012)
22. Y.S. Sung, J.M. Kim, J.H. Cho, T.K. Song, M.H. Kim, T.G. Park, *Appl. Phys. Lett.* **98**, 012902 (2011)
23. R. Zuo, S. Su, Y. Wu, J. Fu, M. Wang, L. Li, *Mater. Chem. Phys.* **110**, 311–315 (2008)
24. J. Chen, J. Cheng, *J. Alloy. Compd.* **589**, 115–119 (2014)
25. W. Yi, Z. Lu, X. Liu, D. Huang, Z. Jia, Z. Chen, X. Wang, H. Zhu, *J. Mater. Sci. Mater. Electron.* (2021). <https://doi.org/10.1007/s10854-021-05490-9>
26. L. Lutterotti, *MAUD, Material Analysis Using Diffraction* (2019). <http://www.ing.unitn.it/~maud/index.html>. Accessed 20 July 2019
27. Y. Wei, X. Wang, J. Zhu, X. Wang, J. Jia, *J. Am. Ceram. Soc.* **96**, 3163–3168 (2013)
28. T. Rojac, M. Kosec, B. Budic, N. Setter, D. Damjanovic, *J. Appl. Phys.* **108**, 74107 (2010)
29. T. Zheng, Y. Ding, J. Wu, *RSC Adv.* **6**, 90831–90839 (2016)

**Publisher's Note** Springer Nature remains neutral with regard to jurisdictional claims in published maps and institutional affiliations.